Proceedings World Geothermal Congress 2000
Kyushu - Tohoku, Japan, May 28 - June 10, 2000

THE MESHKIN SHAHR GEOTHERMAL PROSPECT, IRAN

Ian Bogie[1], A. J. Cartwright[1], Khosrow Khosrawi[2], Behnam Talebi[2] and F. Sahabi[2]
[1]Kingston Morrison Ltd., PO Box 9806, Newmarket, Auckland, New Zealand
[2]SUNA Renewable Energy Organisation of Iran, PO Box 14155-6398, Tehran, Iran

Key Words: Meshkin Shahr, geothermal, Iran, decollement, vapour cored system

ABSTRACT

Mt. Sabalan, an immense trachyandestic stratovolcano with a prominent caldera, hosts a geothermal prospect near the town of Meshkin Shahr in northwest Iran. The volcanic rock chemistry indicates that volcanism has been produced in response to crustal thickening by thrusting; there is no current day subduction. An associated shallow magma chamber beneath the mountain is also indicated by the rock chemistry and Ar-Ar and K-Ar dating.

The volcanic pile sits on an Early Miocene monzonitic batholith in the southwest and Late Miocene sediments in the northeast. Deformation of the sediments by the weight of the volcanic pile has resulted in a very large slump that has displaced the volcanic pile and opened the Moil valley. This has been followed by the extrusion of a small trachydacite dome in the Moil valley that is likely to be derived from an apophysis of the shallow magma chamber. Such an apophysis may represent the heat source of a geothermal system.

Hotspring chemistry indicates that perched groundwater aquifers that exhibit storage behaviour contain neutralised magmatic volatile condensate. Such chemistry is consistent with the presence of the shallow magma chamber inferred from the geology.

A significant area of deep low resistivity indicated by an MT survey is found in the Moil valley but not in the vicinity of the trachydacite dome, possibly due to inherently higher resistivities within a vapour core. Therefore, since the area of deep low resistivity is large an exploitable geothermal system is likely to be present as a neutralised zone around a magmatic vapour core.

1. INTRODUCTION

The Meshkin Shahr geothermal prospect lies in the Moil valley on the western slopes of Mt. Sabalan (Figure 1A), approximately 12 km SE of the town of Meshkin Shahr, in the province of Ardabil in northwest Iran. Mt. Sabalan has been previously explored for geothermal resources in 1978, with geological, geochemical and geophysical surveys being undertaken (Foutohi, 1995). Renewed interest in the area resulted in further geophysical, geochemical and geological surveys being carried out in 1998. These have identified a number of prospects associated with Mt. Sabalan (Sahabi *et al*., 1999). The Meshkin Shahr prospect has been identified as the best of these prospects and is the subject of this paper.

2. REGIONAL GEOLOGY AND TECTONICS

Mt. Sabalan lies on the South Caspian plate, which underthrusts the Eurasian plate to the north (Figure 1B). It is in turn underthrust by the Iranian plate, which produces compression in a northwest direction. This is complicated by a dextral rotational movement caused by northward underthrusting of the nearby Arabian plate beneath the Iranian plate. There is no Benioff-Wadati zone to indicate any present day subduction (McKenzie, 1972).

The Mt. Sabalan volcanic rocks are potassic calcalkaline trachyandesites to rhyolites with high concentration of LIL-elements, plus a high Ni content and a high Ce/Yb ratio (Dostal and Zerbi, 1978). High Ni contents are indicative of a thick crust and are consistent with crustal thickening through underthrusting, but the Ce/Yb ratios are too high for the melts to be derived from typical sialic crust (Gill, 1981). However, such chemistry is consistent with the melts being formed by crustal thickening forcing mantle wedge material, previously metasomatised during prior subduction, below its phlogopite stability depth. Break down of the phlogopite initiates partial melting of the metasomatised mantle wedge to produce a LIL-element enriched melt (Muller and Groves, 1995). The previously metasomatised mantle wedge material was produced during pre-Pliocene subduction. Ratios of FeO*/MgO and Na_2O/K_2O in the volcanic rocks of Mt. Sabalan remain the same with increasing silica content. Al_2O_3, TiO_2, FeO*, MgO and CaO, however, decrease with increasing SiO_2 content. All these features are consistent with the fractional crystallisation of hornblende. K-Ar dating (TBCE, 1978) of the analysed rocks indicate that they become more silicic with decreasing age, with dates ranging from 2.9 to 1.3 Ma. A small dome of trachydacite in the Moil Valley has been dated at 0.9 Ma by Ar-Ar dating. These dates are consistent with the presence of a large, young, comparatively shallow magma chamber beneath Mt. Sabalan.

Igneous activity began in the Eocene with the accumulation of potassic alkalic volcanics upon a sequence of Mesozoic and Paleozoic sediments. They were intruded and thermally metamorphosed by an Early Miocene monzonitic batholith, elongate in a NW-SE direction and exposed on the western ridge of Mt. Sabalan. Significant uplift and erosion of the batholith followed and a sequence of Late Miocene non-marine sediments, were deposited to the SW and SE of the batholith.

Volcanism resumed in the Pliocene, building up the base of the Mt. Sabalan volcano by effusive eruptions of pyroxene trachyandesites, culminating in caldera collapse. Subsequently, there was a hiatus in the volcanism together with initiation of widespread hydrothermal activity, and possibly some erosion. Trachydacite domes were then emplaced on the caldera ring and further eruption of trachyandesites, within this caldera, built up the current summit of Mt. Sabalan. Debris flows, terraces and morraines were deposited on the volcanics, and there was late stage emplacement of a small trachydacite dome in the Moil valley.

The caldera rim is readily discernible on SPOT images as an oblate ellipse with a long dimension of 14 km and a short dimension of 12 km, giving an approximate area of 132 km^2 (Figure 1A). It is more eroded on its western side, where major fault zones are prevalent through the mountain.

A much larger arcuate structure is evident 14 km to the SW of the summit of Mt. Sabalan (Figure 1A). It is likely that this feature is a decollement where the volcanic pile has slumped off the Miocene batholith in response to deformation of the Late Miocene sediments in the NE under the weight of the volcanic pile. This type of deformation of volcanic piles has been reported elsewhere (Van Wyk de Vries and Borgia, 1996). It is likely that the decollement has formed the base of the Moil valley and the movement along it approximates the width of the valley, approximately three kilometres. If so, this would suggest that the dacite domes to the east have been displaced from their intrusive source at depth. In which case the upper part of the caldera rim has also displaced. This is indicated in Figure 1C as the inner caldera margin. This would allow the small dome in the Moil valley to have the same intrusive source but being intruded after, and possibly in response to, movement on the decollement. If this is the case, a shallow intrusive can be expected to be occur beneath the Moil valley. This is similar to the mechanism of collapse proposed by Sillitoe (1994) to explain the telescoping of some intrusion related ore deposits.

Two major NE trending structures occur NW and SE of Mt. Sabalan (Figure 1A). North-south lineations run through Mt. Sabalan and define a northern valley. Parallel lineations are also found on the flanks of Mt. Sabalan. They all occur within the major-fault block defined by the NE-striking faults. Similarly, a set of W-E and WNW striking lineations also appear to be confined to the fault block. These form a major fault zone to the south of the summit of Mt. Sabalan and contain the Meshkin Shahr prospect further to the NW.

3. LOCAL GEOLOGY

Four major units have been identified within the Meshkin Shahr prospect (Figure 1C).

3.1 Valhazir Formation

This formation consists of Pliocene pre-caldera trachyandesitic lava flows, tuffs and pyroclastic breccias with a stratigraphic thickness of at least 2000 m. They are the oldest volcanic rocks mapped in this area, and form the lowermost slopes and ridges of the volcanic complex. They are interpreted to predate the development of the caldera. The lavas occupy the highest stratigraphic and topographic positions and occur as short, thick flows, intercalated with the enclosing tuffs and breccias. They are more fractured and are more affected by faulting than the younger units.

The lavas contain phenocrysts of plagioclase, sanidine, hornblende, biotite and augite in a groundmass rich in plagioclase laths, fine mafics, opaques (magnetite) and glass (where unaltered or not devitrified). Accessory titanite and zircon grains are rare, whereas apatite grains are widespread.

The pyroclastics are fine grained tuffs, rich in feldspar and subordinate mafic crystal fragments. All are at least moderately altered, which means primary textures and minerals are difficult to recognise, but in general, these rocks contain the same minerals in the same proportions as the co-eruptive lavas.

3.2 Toas Formation

These are Pleistocene syn-caldera trachydacitic volcanics associated with the displaced caldera rim comprised of a series of trachydacite and minor trachyandesite and rhyolite flows, domes and lahars. The steep-sided domes have an arcuate distribution interpreted to represent the margin of the inner caldera, and the viscous flows and minor lahars that emanate from them are directed downslope, overlying the pre-caldera volcanics. The northernmost of the Toas Formation volcanics comprise a small dome and an associated extensive and distinctive ropey, trachyandesite flow. The other larger domes, and significantly smaller flows to the southwest are a rhyolite and trachydacites. A small, isolated dome of trachydacite is found near Moil. This dome, which is surrounded on three sides by terrace deposits of the Dizu Formation, is underlain by altered, pre-caldera tuffs. It is petrographically similar to the other trachydacite domes east of the Toas plateau, and on this basis is included in the Toas Formation although is 0.4 Ma younger. It appears to have been erupted up the undisplaced caldera rim.

The northernmost Toas Formation dome and flow is a trachyandesite containing abundant plagioclase and subordinate biotite and hornblende phenocrysts with little or no augite and with minor titanite. In contrast, the southwestern syn-caldera flows and domes are trachydacites and a rhyolite containing phenocrysts of embayed quartz. All of the syn-caldera lavas have glassy, vesicular, strongly flow aligned groundmasses that in some cases has devitrified to spherules of radiating needles of fine cristobalite and K-feldspar.

3.3 Kasra Formation

This formation consists of Pleistocene post-caldera trachyandesitic volcanics largely located outside the mapped area. They form the main peaks of Sabalan, Sabalan Sultan and Kasra to the south and east. These peaks have been formed by a series of trachyandesitic domes and lava flows, together with associated lahars, and they are present (particularly the lava flows and lahars) at the southeastern end of the Meshkin Shahr prospect. They are the products of resurgent volcanism located along the central axis (N-S) of the caldera. The largest trachyandesite lava flows are from Kuh-e-Kasra and one of these is of relatively low viscosity, having flowed downslope in a sinuous path between older trachydacite domes over a distance of 2.5 km. Southeast of this flow, the mountainside rises steeply up to the trachyandesite dome that forms Kuh-e-Kasra. The lahar and lava flows of the Kasra Formation have flowed over the pre-caldera volcanics, but they only partially overlie the topographically higher syn-caldera domes and flows.

The lava flows and domes are all trachyandesites that contain abundant plagioclase and subordinate K-feldspar, biotite, hornblende and augite phenocrysts in a glassy groundmass.

3.4 Dizu Formation

This includes Quaternary alluvium, fans and terrace deposits and thin airfall ash interlayered with thick lahar and debris flows. In part these have been subsequently reworked by fluvial processes to create crudely stratified, terraced deposits up to 150 m thick. In other areas, these terraced deposits form only a thin veneer (less than 10 m) over the volcanics. The clasts (ash, crystal and lithic fragments, and blocks of lava) within the terrace deposits are derived from all three (post-, syn- and pre-) volcanic units.

Fan deposits, large enough to be mapped as discrete rock types, occur in the area, one at the head of the Moil valley and the other in a smaller valley south of Dizu. These thin deposits are debris/mass flows comprised of volcanic boulders, located on steep slopes at close to their angle of repose. The fan deposit south of Dizu appears to be a little older than the one at the head of the main valley, as it is less steep and more vegetated.

A number of areas are covered by thin (up to 10-20 m), elongate, flat-lying lacustrine deposits of sand and pebble sized volcanogenic clasts, which occur in topographic depressions developed by faulting and/or volcanism. These appear to have been created where streams and rivers have built up alluvial deposits and then been choked off, resulting in the formation of a shallow lake. The largest examples are the extensive flats on the Toas plateau and the large plain at Hoshan Medan in the north.

3.5 Hydrothermal Alteration

A 100 km^2 area of hydrothermal alteration was interpreted from SPOT imagery (Figure 1A) with part of it within the Meshkin Shahr prospect. At least in this area essentially all of the hydrothermal alteration is confined to the Valhazir Formation. Within the Valhazir Formation, the original volcanic lithology exerts a major control over the intensity of alteration. The andesite lavas are generally weakly altered or fresh and are only strongly altered close to some fractures. The tuffs and pyroclastic breccias are strongly to intensely altered. In general, the existence of the alteration assemblages described below, is consistent with the development of a widespread, low temperature part of a hydrothermal system. The stratigraphically higher lavas, however, are all unaltered and may have been above the piezometric surface of the hydrothermal system. The secondary minerals found in the weakly altered trachyandesite lavas include smectite, kaolinite, cristobalite, opal, chalcedony, and opaques.

The tuffs and pyroclastic breccias contain abundant quartz and kaolinite, together with minor opaques and alunite. The samples containing alunite constitute advanced argillic alteration assemblages and are likely to have formed under acidic hydrothermal conditions. Those not containing alunite are argillically altered and have probably formed from cool, low salinity, less acid waters. The alteration in the samples containing secondary quartz is relict because secondary quartz can only be found on the surface as a recrystallisation product of older silica, or as deep material exposed by erosion.

However, some samples contain smectite, cristobalite, opal and no quartz, which indicates their alteration may be associated with current thermal activity evident in the near surface. In addition two intensely altered hydrothermal breccias are found as float, one is composed of fine quartz, whereas the other is largely opaline, particularly the breccia matrix that encloses older quartz, hematite and alunite altered clasts.

4.0 SPRING CHEMISTRY

The springs in the Meshkin Shahr prospect issue mainly from the gravels of the Dizu Formation (Figure 1C). There are no springs reported downstream at lower elevations. The Gheynarge, Khosraw-su, Malek-su and Ilando springs produce neutral-Cl-SO_4 waters with up to 1500 ppm Cl and 442 ppm SO_4 and have significant concentrations of Mg (up to 24 ppm). They have a simple dilution trend indicating mixing with varying amounts of shallow groundwater (Table 1). They exhibit a strong seasonal cyclic variation in flow rate but show very little seasonal variation in temperature or chemistry, which is indicative of storage behaviour. Despite the elevated Cl concentration, isotopically the waters lie on the local meteoric water line.

Mg concentrations show little inverse correlation with chloride, suggesting that Mg is high in both the chloride aquifer and the shallow diluting groundwater. Although NaK ratios are low this is likely to reflect the K-rich nature of the country rock and the KMg cation geothermometer is therefore the most appropriate to use. The least diluted analysis that contains tritium at below detection limit and therefore contains no young groundwaters gives a KMg temperature of 131°C in reasonable agreement with the chalcedony geothermometer temperature of 135°C (Table 2).

The Moil, Moil 2, Aghsu and Romy springs are acid (pH 4.28, 3.20, 3.53 and 2.76 respectively). The Moil 2 and Agsu springs are typical acid-SO_4 waters and therefore have formed by condensation and oxidation of H_2S, implying boiling at greater depths. The Moil springs have been slightly neutralised and are therefore further from the source of H_2S than the Moil 2 springs. The Romy spring waters contain significant Cl (119 ppm). It is difficult to derive a water of this temperature and chemistry by mixing of the other spring chemistries and it is possible that the Romy spring waters may represent a diluted but un-neutralised equivalent of the neutral Cl-SO_4 waters.

The storage behaviour of the springs is indicative of them being fed by very large perched groundwater aquifers. To be heated and to obtain a high Mg neutral Cl-SO_4 composition requires that magmatic volatiles have condensed and been neutralised within these aquifers. A degassing shallow intrusive and possible heat source is therefore inferred which is consistent with a similar conclusion from the geology. The acid-SO_4 chemistry of the Agsu and Moil 2 springs may be the result of unrelated localised boiling, condensation, and oxidation of H_2S. However, their location at different elevations either side of the trachydacite dome two kilometres apart is suggestive that they are derived from a convective zone around such an intrusion. Thus, the intrusion is likely to lie between the springs near the trachydacite dome.

5. MT SURVEY

An MT Survey (Bromley *et al*., in prep.) has identified a large, low resistivity area that includes the Moil valley. A certain proportion of this low resistivity will be from argillic alteration in the Valhazir Formation. Deep low resistivities

are restricted to the Moil Valley with a strong structural boundary indicated in the north from anistropic effects on the MT results. Shallow low resistivities in the Moil valley correspond well with the distribution and thickness of the gravels and these correspond to the condensate bearing groundwater aquifers indicated by the spring geochemistry. The deep low resistivities are not found in the entire valley and most particularly they are not present near the trachydacite dome and its surrounds. This may simply mean that the dome is unrelated to the thermal activity. However, if this area at depth corresponds to a degassing intrusive it is possible that a vapour-cored system (Giggenbach *et al*., 1990) is present. If so, it is likely to be at high temperatures where magmatic volatiles are poorly dissociated and hence poorly conductive and there are limited conductive alteration minerals present. Therefore, the central part of such a system may not have low resistivities at depth. The surrounding area of low resistivity at depth may therefore correspond to a zone of condensation and neutralisation of magmatic volatiles immediately around the vapour core with a convecting exploitable geothermal resource being found further away from the dome.

6. CONCLUSIONS

Low apparent resistivities are found at depth in the Moil valley where both geological and geochemical evidence is suggestive of a shallow intrusive being present. Groundwater aquifers containing neutralised magmatic volatiles and the pattern of low resistivities at depth implies that a vapour cored geothermal system may be present. Such systems have been explored for geothermal energy (Reyes *et al*., 1993) but have only been successfully developed where they are sufficiently large and evolved that high temperatures exist outside of the vapour core. In these cases the vapour core can be avoided and the surrounding neutralised zone or outflow exploited, for example Mt. Apo in the Philippines (Sambrano, 1998). As a large area of low resistivity at depth has been identified at the Meshkin Shahr prospect, it is considered likely that the system is large enough for an exploitable geothermal system to be present (Figure 2).

ACKNOWLEDGEMENTS

A review of this paper by P. R. Barnett and J.V. Lawless is much appreciated and the permission for SUNA to present this paper is gratefully acknowledged.

REFERENCES

Dostal, J. and Zerbi, M. (1978). Geochemistry of the Savalan Volcano (Northwestern Iran). *Chemical Geology, Vol.*22, pp. 31-42.

ENEL (1983). Geothermal power development studies in Iran, General Report on Sabalan Zone. *Report to Ministry of Energy, Islamic Republic of Iran.*

Fotouhi, M. (1995). Geothermal development in Sabalan, Iran. *Proceedings of the World Geothermal Conference, Florence* Vol.1, pp. 191-196.

Fournier, R.O. (1979). A revised equation for the Na/K geothermometer. *GRC Transactions* 3, pp. 221-224.

Giggenbach, W.F. (1988). Geothermal solute equilibria. Derivation of Na-K-Mg-Ca geoindicators. *Geochimica et Cosmochimica Acta* 52, pp. 2749-2765.

Giggenbach, W.F., Garcia, N., Londono, A., Rodriguez, V., G. Rojas N. and Calvache, M.L. (1988). The chemistry of fumarolic vapor and thermal-spring discharges from the Nevado del Ruiz volcanic-magmatic hydrothermal system, Colombia. *Journal of Volcanology and Geothermal Research*, Vol., 42, pp. 13-39.

Gill, J.B. (1981). *Orogenic andesites and plate tectonics. Springer-Verlag*, Berlin, Heidelberg, New York.

McKenzie, D.S. (1972). Active tectonics of the Mediterranean region. *Geophys. J. R. Astr.Soc*., Vol. 30, pp. 109-185.

Muller, D. and Groves, D.I. (1995). *Potassic igneous rocks and associated gold-coppper mineralisation*. Springer-Verlag, Berlin.

Reyes, A.G., Giggenbach, W.F., Salera, J.R.M., Salonga, N.D. and Vergara, M.C. (1997). Petrology and geochemistry of Alto Peak, a vapor-cored hydrothermal sytem, Leyte Province, Philippines. *Geothermics* Vol. 22, pp. 479-520.

Sahabi, F., Khoshlessan, M.R. and Barnett, P. R. (1999). Geothermal exploration of Mount Sabalan, NW Iran. *Proceedings 1999 GRC Conference.*

Sambrano, B.M. (1998). Fluid-mineral equilibria of fluids from production wells of the Sandawa sector, Mt. Apo, Philippines. *Proceedings 19th Annual PNOC-EDC geothermal conference*, pp. 21-37.

Sillitoe, R.H. (1994). Erosion and collapse of volcanoes: Causes of telescoping in intrusion-centred ore deposits. *Geology* Vol., 22, pp. 945-948.

TBCE (1979). Geothermal power development studies, Sabalan Zone. *Report to Ministry of Energy, Islamic republic of Iran.*

Van Wyk de Vries, B. and Borgia, A. 1996. The role of basement in volcano deformation. *Geological Society Special Publication* No. 110, pp. 95-110.

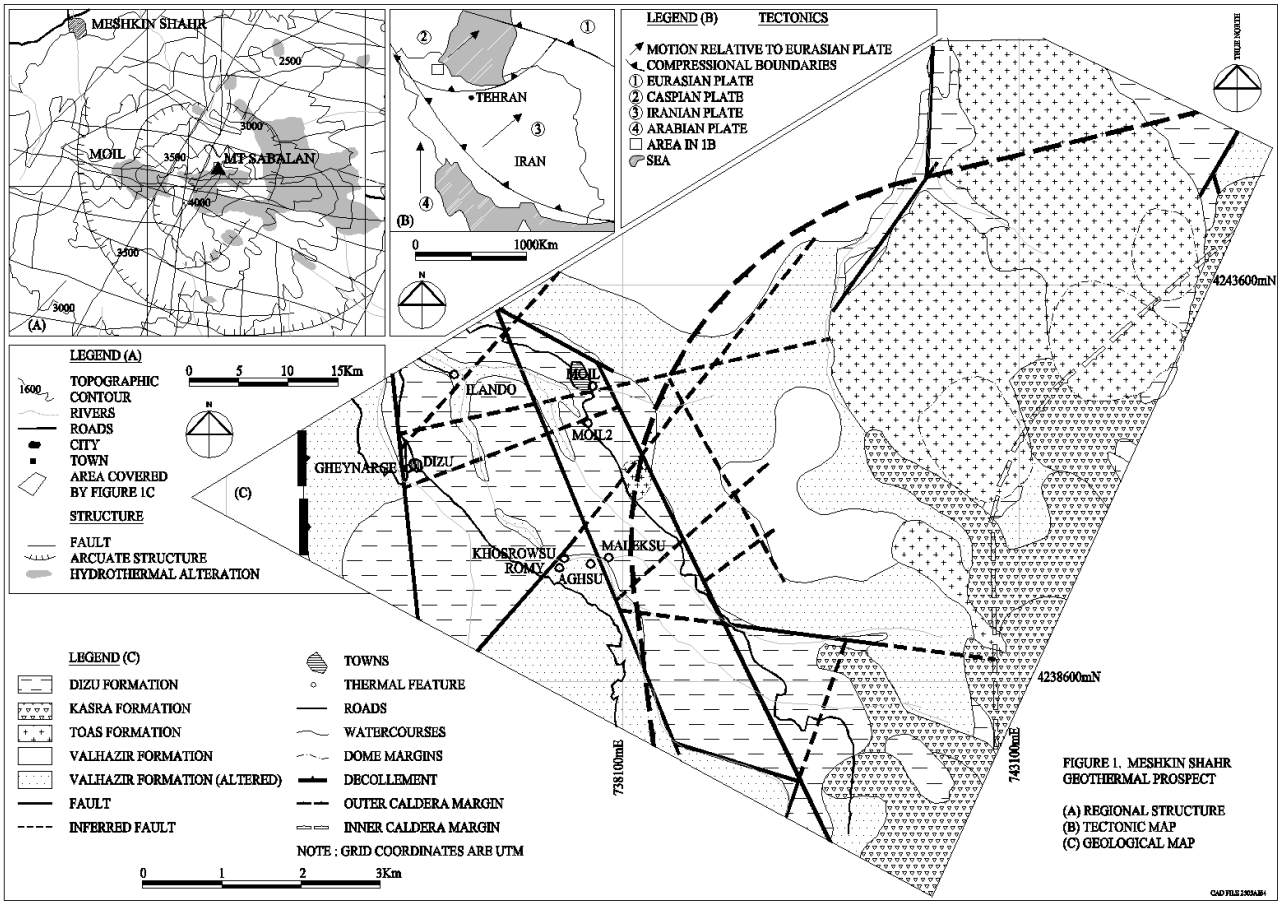

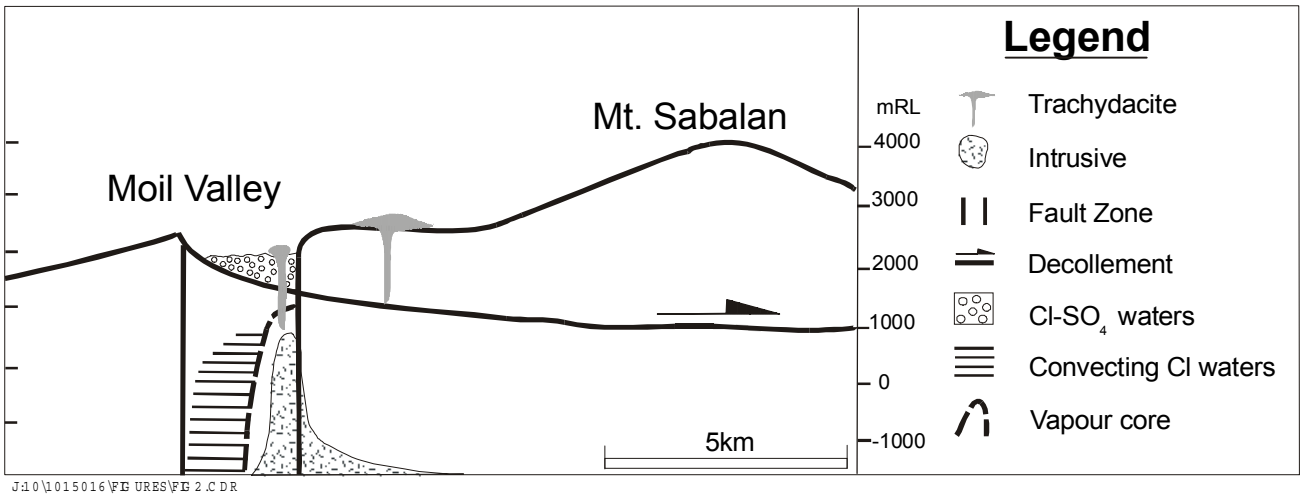

J:\10\1015016\FIGURES\FIG2.CDR

Figure 2 Conceptual Model

Table 1: Hotspring chemistry and isotope data

Source	Name	Date	Elev	Flow	Temp	pH	Li	Na	K	Ca	Mg	Rb	Cs	Cl	F	SO_4	HCO_3	B	SiO_2	NH_3	$S^=$	tCO_2	TDS	^3H	$\delta^{18}O$	δD
			m	l/min	°C											ppm								TU	‰	‰
TBCE (1979)	Ilando	20-Aug-77		8	37	6.00	0.69	322	43.0	80.2	19.4	0.24	1	425	1.0	283	165	3.4	154	<11	<3.1	365	1464	6.3	-10.2	-71.9
TBCE (1979)	Ilando	24-May-78		2500	37	6.40	1.53	276	39.1	72.1	20.7	0.44	0	390	1.2	288	153	3.4	160	<11	<3.1	680	1381	-	-10.3	-71.3
ENEL (1983)	Ilando	1-Sep-75		-	37	6.10	1.32	3	430.1	78.2	21.9	0.30	0	425	-	293	146	0.0	140	0.0	0.0	380	1800	4.6	0.0	-
This study	Ilando	10-Sep-98	2000	-	36	6.04	1.30	304	38.0	72.0	20.3	0.20	0	381	-	281		3.4	141	-	-	299	-	-	-	-
TBCE (1979)	Gheynarge	20-Aug-77		1000	84	6.80	1.39	690	105.6	124.2	21.9	0.94	3	957	1.3	432	171	7.8	128	0.3	<3.1	51	2610	<1.1	-9.8	-72.5
TBCE (1979)	Gheynarge	24-May-78		100	85	6.40	3.12	690	109.5	130.3	24.3	1.37	1	993	1.7	442	159	8.6	130	<11	<3.1	440	2618	-	-10.1	-72.3
ENEL (1983)	Gheynarge	1-Sep-75		-	81	6.50	0.02	897	148.6	110.0	18.2	1.54	-	1,489	-	298	67	11.9	145	0.0	-	170	3200	0.0	-10.0	-
This study	Gheynarge	10-Sep-98	2124	-	84	6.84	4.70	1045	116.0	107.0	15.6	0.87	1	1,541	-	300	-	12.6	134	-	-	216	-	-	-	-
This study	Khosraw-su	10-Sep-98	2164	-	68	6.39	2.70	748	90.0	99.0	20.3	0.54	1	1,147	-	172	-	9.3	104	-	-	285	-	-	-	-
This study	Malek-Su	10-Sep-98	2153	-	46	6.17	0.25	184	35.0	31.0	14.6	0.12	0	251	-	81	-	2.1	106	-	-	252	-	-	-	-
This study	Romy	10-Sep-98	1904	-	21	2.76	0.34	93	12.3	88.0	44.0	0.09	0	119	-	753	-	1.0	52	-	-	-	-	-	-	-
This study	Agsu	10-Sep-98	2320	-	36	3.53	<0.05	20	12.3	31.0	5.1	0.06	<0.05	5	-	154	-	0.0	117	-	-	<10	-	-	-	-
TBCE (1979)	Moil	21-Aug-77		30	45	5.70	0.01	80	30.1	92.2	24.3	0.09	0	2	1.0	480	2	0.1	26	<11	<3.1	365	878	<1.0	-11.2	-73.5
TBCE (1979)	Moil	25-May-78		200	44	5.30	0.03	80	30.1	96.2	25.5	0.17	0	1	1.3	480	25	0.1	28	<11	<3.1	680	813	-	-11.5	-73.7
This study	Moil	13-Sep-98	2183		46	4.28	<0.05	79	27.0	98.0	27.0	0.09	<0.05	1	-	528	-	<0.1	27	-	-	241	-	-	-	-
TBCE (1979)	Moil 2	21-Aug-77		12	15	6.80	<0.58	13	5.5	28.1	5.2	0.01	0	6	1.0	33	73	0.1	60	<11	<3.1	30	258	-	-10.9	-76.9
TBCE (1979)	Moil 2	25-May-78		10	46	4.28	0.00	11	5.0	28.0	5.3	0.09	<0.015	7	0.4	48	67	0.0	56	<11	<3.1	60	209	-	-12.0	-75.6
This study	Moil 2	13-Sep-98	2153		30	3.20	<0.05	29	10.1	45.0	11.2	<0.05	<0.05	1	-	330		<0.1	30	-	-	-	-	-	-	-

Table 2. Molar ratios and geothermometry temperatures

Source	Name	Date	Cl / Li	Cl / Ca	Cl / B	Cl / SO_4	Cl / HCO_3	Cl / Mg	Na / K	Na / Ca	HCO_3 / SO_4	QTZ (A) °C	QTZ (B) °C	CHAL °C	AM °C	NaK (F 79) °C	NaK (G 88) °C	KMg °C	TNaKCa ß	TNaKCa °C	TMg °C	ΣCATS meq	ΣANS meq
TBCE (1979)	Ilando	20-Aug-77	121	6.0	39	4.07	4.44	15.00	12.7	7.0	0.9	154	163	139	40	243	257	94	0.33	196	76	20.7	20.7
TBCE (1979)	Ilando	24-May-78	50	6.1	35	3.67	4.40	12.94	12.0	6.7	0.8	156	165	142	42	249	262	90	0.33	197	66	18.3	19.6
ENEL	Ilando	1-Sep-75	63	6.2	-	3.93	5.00	13.33	0.0	0.1	0.8	149	157	133	35	-	-	165	0.33	1181	952	16.8	20.5
This study	Ilando	10-Sep-98	57	6.0	34	3.67	-	12.87	13.6	7.4	-	150	157	133	35	237	251	90	0.33	192	66	19.5	16.6
TBCE (1979)	Gheynarge	20-Aug-77	135	8.7	37	6.00	9.64	30.00	11.1	9.7	0.6	145	151	126	30	256	269	117	0.33	215	112	40.7	38.9
TBCE (1979)	Gheynarge	24-May-78	62	8.6	35	6.09	10.77	28.00	10.7	9.2	0.6	145	152	127	31	260	272	117	0.33	217	108	41.3	39.9
ENEL (1983)	Gheynarge	1-Sep-75	14994	15.3	38	13.55	38.18	56.00	10.3	14.2	0.4	151	159	135	37	264	276	131	0.33	227	133	49.8	49.3
This study	Gheynarge	10-Sep-98	64	16.3	37	13.92	-	67.72	15.3	17.0	-	147	154	130	32	226	241	125	0.33	205	127	55.0	49.7
This study	Khosraw-su	10-Sep-98	83	13.1	38	18.07	-	38.74	14.1	13.2	-	135	139	113	19	233	248	114	0.33	204	99	41.4	35.9
This study	Malek-Su	10-Sep-98	196	9.2	36	8.40	-	11.79	8.9	10.3	-	135	140	114	20	279	289	92	0.33	215	52	11.6	8.8
This study	Romy	10-Sep-98	68	1.5	36	0.43	-	1.85	12.9	1.8	-	104	104	74	-12	242	256	54	1.33	72	46	14.1	19.0
This study	Agsu	10-Sep-98	-	0.2	34	0.08	-	0.60	2.8	1.1	-	140	146	120	25	-	-	79	1.33	78	-	3.5	3.3
TBCE (1979)	Moil	21-Aug-77	25	0.0	7	0.01	1.55	0.05	4.5	1.5	0.0	78	74	42	-38	364	365	82	0.33	230	73	10.9	10.1
TBCE (1979)	Moil	25-May-78	6	0.0	6	0.01	0.08	0.03	4.5	1.5	0.1	81	77	45	-35	364	365	81	1.33	99	67	11.2	10.5
This study	Moil	13-Sep-98	-	0.0	-	0.01	-	0.03	5.0	1.4	-	79	75	44	-36	351	354	78	1.33	94	66	11.3	11.0
TBCE (1979)	Moil 2	21-Aug-77	-	0.2	18	0.49	0.14	0.79	4.1	0.8	3.5	110	111	81	-7	-	-	60	1.33	52	-	2.5	2.1
TBCE (1979)	Moil 2	25-May-78	-	0.3	70	0.38	0.17	0.87	3.7	0.7	2.2	107	107	78	-9	-	-	58	1.33	48	-	2.5	2.3
This study	Moil 2	13-Sep-98	-	0.0	-	0.01	-	0.08	4.9	1.1	-	83	79	48	-33	-	-	65	1.33	68	-	5.3	6.9

(A) Adiabatic
(B) Conductive
(F 79) Fournier (1979)
(G 88) Giggenbach (1988)